

# A Dynamic Light Scattering Study of Fast Relaxations in Polymer Solutions

P. Štěpánek,\* Z. Tuzar, P. Kadlec, and J. Kříž

*Institute of Macromolecular Chemistry, Academy of Sciences of the Czech Republic, Prague, Czech Republic*

*Received September 5, 2006; Revised Manuscript Received January 10, 2007*

**ABSTRACT:** We have analyzed the fine structure of the distribution of relaxation times obtained from dynamic light scattering on solutions of homopolymers and diblock copolymers. We have shown that in a carefully designed experiment two additional fast modes can be identified in the distribution of relaxation times, besides the usual cooperative mode, heterogeneity mode, and cluster mode. We have shown that the faster of these two modes, well observable only at small angles, is due to the thermal diffusion coefficient of the solvent. For the slower of these two modes, several experimental findings lead to the conclusion that this mode is representative of the motion of the solvent molecules in the solution.

## 1. Introduction

Dynamic light scattering has now been used for more than 30 years in experimental studies of dilute, semidilute, and concentrated polymer solutions, and many aspects of this powerful technique have been investigated in various systems. In the pioneering days linear correlators have been used with a relatively low number of channels (16–64) that still made it possible to determine the translational diffusion coefficient in particle dispersions or dilute polymer solutions with good accuracy.<sup>1</sup> Soon it became apparent that when more complicated systems than dilute solutions are examined, the correlation function cannot be described by a single relaxation time but several components are needed. When the ratio of relaxation times was larger than 3–5, splicing of correlation curves was applied to generate a combined correlation function covering a larger interval of delay times.<sup>2,3</sup> Continuing advances in this field lead to construction of logarithmic multi- $\tau$  correlators<sup>4</sup> covering a dynamic range of a few or many decades of delay time. It has been shown that the detailed information contained in correlation functions with channels linearly spaced over the whole delay time range was not needed.<sup>5–7</sup> Progress in electronics over the years has made correlators still faster and photon detection more efficient. The fastest correlators today offer a shortest delay time of a few nanoseconds while the longest delay time depends on the measurement time and is almost unlimited. Practical accumulation times rarely exceed 1 or 2 days above which difficulties may appear with sample or instrument stability or operator's patience.

A large number of different dynamic processes have been described in various polymer–solvent systems which have been reviewed in recent years.<sup>8–10</sup> Important examples are the following: (1) In dilute solutions: translational diffusion of polymer coils, internal mode of homopolymer,<sup>11</sup> or diblock copolymer chains.<sup>12,46,47</sup> (2) In semidilute solutions: cooperative diffusion of the transient polymer network, heterogeneity mode related to polymer self-diffusion (in diblock copolymers),<sup>12,13,17,46,47</sup> entanglement mode,<sup>14</sup> chain reptation,<sup>14,15</sup> viscoelastic relaxation,<sup>16</sup> diffusion of clusters.<sup>13,17,18,36</sup> Rouse modes have been predicted theoretically<sup>19</sup> and observed experimentally.<sup>20</sup> (3) In

concentrated solutions: viscoelastic relaxations,  $\alpha$ - and  $\beta$ -chain relaxations.<sup>16,21,22</sup>

While from a physical point of view these dynamic processes exist in any polymer solution, some of them are not observable or detectable under given conditions due to the properties of the light scattering process (insufficient contrast or scattering amplitude) or due to the dynamical range of the dynamic light scattering technique (the process is too fast to be detected).

Dynamic light scattering has been used independently in a different field of dynamic properties of pure liquids or binary mixtures of liquids. Thus, it has been shown that the thermal diffusion coefficient of pure liquids can be determined when a heterodyne dynamic light scattering measurement is performed at very small angles.<sup>23,24</sup> The thermal diffusion coefficient has also been determined in glass-forming liquids by dynamic light scattering<sup>25,26</sup> and by forced Rayleigh scattering.<sup>26,27</sup> The mutual diffusion coefficient of binary mixtures has been studied on the systems methanol/benzene and ethylacetate/cyclohexane<sup>28,29</sup> and in several other mixtures of simple organic liquids.<sup>30</sup>

In this paper we report on dynamic light scattering experiments performed on a number of polymer–solvent systems that have been initiated by our ongoing investigation of dynamic properties of self-organized diblock copolymer systems in mixtures of two partially miscible solvents.<sup>31</sup> In these studies we observe, besides the dominant polymer diffusion process and the slower modes described previously, also two additional diffusive modes with relaxation times smaller than those corresponding to the translational or cooperative diffusion. Here we show that one of these processes corresponds to the solvent thermal diffusion, and we present speculations on the origin of the other fast mode.

## 2. Theory

We follow the derivation of some aspects of the dynamic light scattering theory as presented in refs 11 and 32 with several details that will be useful in the discussion below. The intensity of light of frequency  $\omega$  scattered with a scattering vector  $q$ ,  $I(q, \omega)$ , is given by the fluctuations of dielectric constant  $\epsilon$ . We consider a binary mixture of two components such as a mixture of two liquids or a mixture of a polymer and a solvent. The dielectric constant of such a medium fluctuates because of fluctuations in temperature  $T$ , pressure  $p$ , and concentration  $c$ :

\* Corresponding author. E-mail: stepan@imc.cas.cz.

$$d\epsilon(q, \omega) = \left( \frac{\partial \epsilon(q, \omega)}{\partial c} \right)_{T, P} dc + \left( \frac{\partial \epsilon(q, \omega)}{\partial T} \right)_{c, P} dT + \left( \frac{\partial \epsilon(q, \omega)}{\partial P} \right)_{T, c} dP \quad (1)$$

Fluctuations in temperature lead to the thermal diffusion coefficient  $D_T$ , observed in pure solvent,<sup>23–27</sup> fluctuations in pressure to frequency-shifted peaks in the frequency spectrum of scattered light that are related to the speed of sound, and fluctuations in concentration to the mutual diffusion coefficient  $D$  of the polymer/solvent system.

### 3. Experimental Section

**3.1. Materials.** The polymers used were (1) a diblock copolymer polystyrene-*b*-poly(ethylene-propylene), a commercial product of Shell Co. labeled as SV-50 with molecular weight  $M_w = 96\,000$ , polydispersity  $M_w/M_n < 1.2$ , and styrene weight fraction  $f = 0.43$ , and (2) a polystyrene standard PS-97 (Polymer Source Inc.) with molecular weight  $M_w = 97\,000$ , with  $M_w/M_n = 1.05$ . The solvents toluene and tetrahydrofuran (THF) of p.a. grade were purchased from Aldrich and used as received.

The solutions of polymers and copolymers were prepared in two steps. A solution in cyclopentane with  $c < c^*$  was prepared and filtered through a  $0.2\,\mu\text{m}$  Millipore filter into a dedusted optically clean sample cell. After evaporation of cyclopentane and drying in vacuo, the final solvent (toluene, THF) was filtered into the cell, which was then flame-sealed. The solution concentrations are indicated in weight percent (wt %).

**3.2. Dynamic Light Scattering.** The dynamic light scattering (DLS) instrument consists of an ALV CGE photogoniometer equipped with a Uniphase 22 mW HeNe laser and an ALV6010 correlator. For measurements at angles below  $15^\circ$  a home-built DLS instrument was used equipped with single-mode fiber optics and an ALV5000/E correlator. In this instrument a 100 mm path length optical cell is used so that measurements down to an angle of  $0.8^\circ$  are possible. For very long measurement times (several hours) an occasional passage of a dust particle (which can never be removed completely) through the scattering volume is unavoidable. To improve the quality of the measurements, a large number of short time accumulations were performed (between 500 and 1000 measurements of 1 min), measurements affected by dust particles were excluded, and the remaining correlation functions were summed and averaged to produce data unaffected by dust. All measurements have been performed at  $25^\circ\text{C}$ .

The measured intensity correlation function  $g^{(2)}(t)$  is related to the field correlation function  $g^{(1)}(t)$  by the Siegert relation<sup>11</sup>

$$g^{(2)}(t) = 1 + \beta |g^{(1)}(t)|^2 \quad (2)$$

where  $t$  is the delay time of the correlation function and  $\beta$  is an instrumental parameter. The field correlation function  $g^{(1)}(t)$  is related to the distribution  $A(\tau)$  of relaxation times  $\tau$  by the Laplace transformation

$$g^{(1)}(t) = \int A(\tau) \exp(-t/\tau) d\tau \quad (3)$$

In order to extract from the measured intensity correlation function  $g^{(2)}(t)$  the distribution of decay times  $A(\tau)$ , we use the nonlinear program REPES<sup>33,34,37</sup> that performs the inverse Laplace transformation of  $g^{(2)}(t)$  according to

$$g^{(2)}(t) = 1 + \beta \left[ \int A(\tau) \exp(-t/\tau) d\tau \right]^2 \quad (4)$$

Since a logarithmic  $\tau$ -axis is used for all  $A(\tau)$  graphs shown below, the distributions of relaxation times are shown in the equal area representation,<sup>34</sup>  $\tau A(\tau)$  vs  $\log \tau$ . The relaxation time  $\tau$  is related to the diffusion coefficient  $D$  by the relation  $D = (\tau q^2)^{-1}$ , where  $q$  is the scattering vector. The hydrodynamic radius  $R_h$  of the diffusing objects is calculated from the diffusion coefficient using the

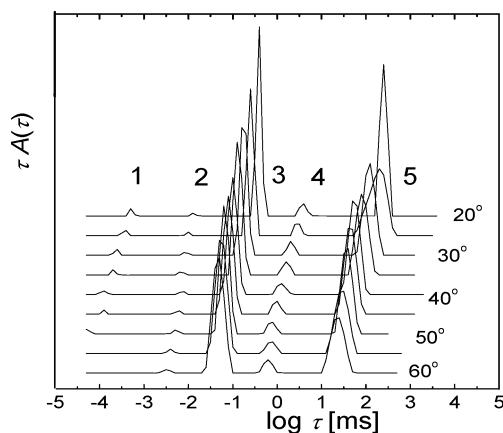


**Figure 1.** Distribution of decay times for a 5 wt % solution of SV-50 in THF at  $25^\circ\text{C}$  and for the indicated scattering angles.

Stokes–Einstein equation

$$D = k_B T / 6\pi\eta R_h \quad (5)$$

where  $T$  is absolute temperature,  $\eta$  the viscosity of the solvent, and  $k_B$  the Boltzmann constant.

For visualization and analysis of some correlation curves we use the subtraction technique developed earlier and fully described in refs 35 and 36. This technique is very useful for the identification and analysis of very weak contributions to the correlation function and for removing some artifacts that may appear in the Laplace transformation process (see eq 4), in particular the so-called  $\delta$ -effect.<sup>37,38</sup> It consists of subtracting from the experimental  $g^{(1)}(t)$  a calculated correlation function  $g_c^{(1)}(t) = \sum_{i=k}^l A_i \exp(-t/\tau_i)$  corresponding to the relaxation times  $\tau_i$  with amplitude  $A_i$  that have to be eliminated, so that

$$g_s^{(1)}(t) = g^{(1)}(t) - g_c^{(1)}(t) \quad (6)$$

**3.3. Pulsed-Field Gradient NMR.** Self-diffusion PFG NMR experiments were measured at  $25^\circ\text{C}$  with an upgraded Bruker Avance DPX300 spectrometer using a  $z$ -gradient inverse-detection diffusion probe connected to a BGu2 gradient unit. A Tanner pulsed-gradient stimulated echo sequence was used with the field-gradient incremented in the range 0–60 G/cm for the solvent self-diffusion and 0–650 G/cm for the polymer self-diffusion. The lengths of the gradient pulses  $\delta$  as well as the diffusion delay  $\Delta$  were held constant, 1 and 60 ms, respectively. The 8K points of the FIDs for each of the 16 experimental points were detected in a quadrature mode and converted to 4K points of the spectra after Fourier transform. The signal intensity decay was fitted to the exponential dependence on the square of gradient magnitude  $g$

$$I(g)/I(0) = \exp[-\gamma^2 D_{s,\text{NMR}} \delta^2 (\Delta - \delta/3) g^2] \quad (7)$$

where  $\gamma$  is the gyromagnetic ratio of protons and  $D_{s,\text{NMR}}$  is the fitted self-diffusion coefficient. All decays for the solvent in the measured systems were strictly monoexponential, offering thus a single value of  $D_{s,\text{NMR}}$ . In the case of the polymer, they were slightly polyexponential due to molecular weight distribution, but the fitting offered one strongly prevailing component (over 90%), which was taken as the value of  $D_{s,\text{NMR}}$ .

### 4. Results

In this contribution we present results obtained in simple systems consisting of (a) one diblock copolymer in a single solvent, (b) one homopolymer in a single solvent, and (c) one neat solvent only.

**4.1. Diblock Copolymer in a Good Solvent.** Figure 1 shows a typical example of distribution of relaxation times obtained

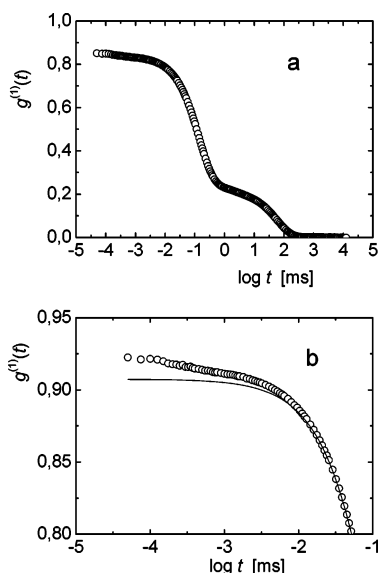


**Figure 2.** (a) Correlation function  $g^{(1)}(t)$  for a 5 wt % solution of SV-50 in THF at 25 °C and scattering angle 30°. (b) Enlarged part of  $g^{(1)}(t)$  in (a) at small delay times  $t$ . The full line corresponds to a correlation function that represents modes 3–5 in Figure 1.

under good solvent conditions on a solution of diblock copolymer SV-50 in THF, a good solvent for both blocks, at 25 °C, the polymer concentration being 5 wt %, at several angles in the range 20–60°. A typical correlation curve is shown in Figure 2a.

In a single good solvent, the diblock copolymer solution is not structured if the concentration is lower than the concentration  $c_{\text{ODT}}$  corresponding to the order-to-disorder transition (ODT). By analogy with results reported in ref 48, we expect that for the polymer SV-50  $c_{\text{ODT}}$  is about 38 wt %. For the data shown in Figure 1 we have  $c < c_{\text{ODT}}$ , and therefore this solution has the properties of a regular semidilute solution.<sup>39</sup> The overlap concentration  $c^*$  (for a homopolymer in a good solvent) can be estimated as<sup>39</sup>  $c^* = M/((4/3)\pi N_A R_g^3)$ , where  $M$  is the molecular weight of the polymer,  $R_g$  the radius of gyration, and  $N_A$  the Avogadro number. For such a polymer we obtain  $c^* = 2$  wt %, and for the solution shown in Figure 1 we have  $c/c^* = 2.5$ . Several modes are visible, numbered from the fastest to the slowest. The decay rate of all modes has been found to be proportional to  $q^2$ ; thus, they can be considered as diffusive. The dominant mode 3 corresponds to classical process of cooperative diffusion of the semidilute solution and has been studied in countless contributions in the past decades (e.g., refs 40 and 41). Using the Stokes–Einstein relation for semidilute solutions

$$D = \frac{k_B T}{6\pi\eta\xi_h} \quad (8)$$

where  $k_B$  is the Boltzmann constant,  $T$  the absolute temperature, and  $\eta$  the solvent viscosity, we obtain for the correlation length (or mesh size)  $\xi_h = 4.3$  nm, which is a typical value for semidilute solutions.<sup>41</sup> Mode 4 is the heterogeneity mode (closely related to self-diffusion of the diblock copolymer chain) which was observed by Balsara et al.<sup>42</sup> and Anastasiadis et al.<sup>43</sup> and theoretically described by Semenov.<sup>46,47</sup> The relative amplitude of mode 5 increases substantially at small scattering angles; thus, it corresponds to diffusion of objects with size comparable to or larger than  $q^{-1}$ . Applying the Stokes–Einstein relation to the relaxation rate of mode 5, we obtain an estimate for the hydrodynamic size of this object  $R_h = 120$  nm. This

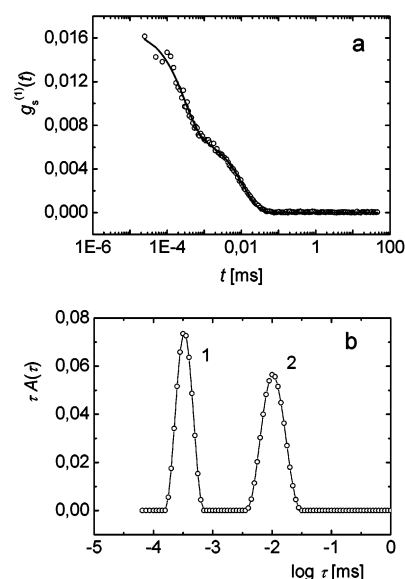


**Figure 3.** (a) Correlation function  $g_s^{(1)}(t)$  from Figure 2a, after subtraction of modes 3–5, using the subtraction technique.<sup>35,36</sup> (b) Distribution of decay times corresponding to (a).

rather slow diffusive mode has been observed a number of times in various polymer systems and is usually referred to as cluster of which typical sizes appear to be about 100–200 nm.<sup>13,17,18,36</sup> For solutions of diblock copolymers its existence has been plausibly explained by Lodge,<sup>44</sup> who argues that even in a solvent that is good for both blocks the interaction between the blocks leads to a tendency of the system to create clusters.

The purpose of this contribution is to discuss in particular the origin and properties of the fast modes 1 and 2 in Figure 1. These modes are not an artifact of the inverse Laplace transformation as demonstrated below. Figure 2a shows the correlation function  $g^{(1)}(t)$  corresponding to one of the distributions (at angle 30°) shown in Figure 1. Figure 2b shows an enlarged view of the initial part of  $g^{(1)}(t)$  where clearly the faster decays are observed. Indeed, the full line represents a correlation function corresponding to modes 3–5 in Figure 1, and a clear and relatively important increase of the experimental data points above this line is observed for delay times  $t$  smaller than 0.01 ms. For a better visualization of this initial decay, Figure 3a shows a correlation function  $g_s^{(1)}(t)$  obtained by subtracting from  $g^{(1)}(t)$  the contributions due to modes 3–5, i.e., a correlation function that would be observed if processes 3–5 did not exist (or for some reason not visible in a light scattering experiment). Figure 3a shows that even if the amplitudes of peaks 1 and 2 in Figure 1 are very small (e.g., 1.2% and 0.7%, respectively, at angle 30°), they are still described by a well-developed correlation function consisting of at least 50 data points. The feasibility of identifying and analyzing components with very small amplitude (0.3%) was demonstrated previously by Pusey et al.<sup>45</sup> Figure 3b shows the distribution of decay times corresponding to  $g_s^{(1)}(t)$  in Figure 3a.

The amplitude of the dominant mode 3 (cooperative mode) in Figure 1 can be substantially decreased by usage of the “zero-average contrast” (ZAC) solvent, meaning that the relative amplitude of the other relaxation processes in the distribution increases and their quantitative assessment is made easier. It has been shown theoretically<sup>46,47</sup> that for diblock copolymer solutions in good solvent the field correlation function can be written as

$$g^{(1)}(t) = A_I \exp(-\Gamma_I t) + A_C \exp(-\Gamma_C t) + A_H \exp(-\Gamma_H t) \quad (9)$$

where  $\Gamma = \tau^{-1}$  is the relaxation rate and C stands for the cooperative mode, I for the internal mode, and H for the heterogeneity mode. The amplitude of the cooperative mode is given by

$$A_C \approx (\langle n \rangle^2 - n_s^2) c N \quad (10)$$

A “zero-average contrast” solvent has a refractive index  $n_s$  equal to the average  $\langle n \rangle$  of the refractive indexes of the two blocks so that  $n_s = \langle n \rangle$ , and then  $A_C$  in eq 9 vanishes. The internal mode predicted in eq 9 is not visible under the conditions of our experiment. Indeed, its amplitude  $A_I$  is predicted<sup>47</sup> to be small and is given by

$$A_I = (n_A^2 - n_B^2)^2 c N (q R_g)^2 \quad (11)$$

It is thus proportional to  $(q R_g)^2$ , which is very small at the small scattering angles used in this work and a relatively small molecular weight of the polymer SV-50. Indeed, it has been observed earlier on a similar polymer–solvent system<sup>48</sup> that the ratio of amplitudes of the internal and heterogeneity modes is approximately  $A_I/A_H = 0.1$  at angle  $90^\circ$ ; at angle  $20^\circ$  this ratio would be 16 times smaller, thus of the order of 0.005. The decay rate of the internal mode is predicted to be independent of the scattering vector  $q$ . No  $q$ -independent modes have been observed in the data presented below. The theory<sup>46,47</sup> leading to eq 9 refers only to polymer chains; therefore, it does not include the fast modes 1 and 2 and the cluster mode 5 in Figure 1.

It appears that neat toluene is an almost “zero average contrast” solvent for the PS–PEP diblock copolymer of comparable block lengths. Figure 4 shows that a similar distribution of relaxation times is obtained for the same sample dissolved in toluene, as is shown in Figure 1 for THF. Mode 3 now has much smaller amplitude although it does not vanish. Indeed, in this case  $\Delta n \sim (\langle n \rangle - n_s) \sim dn/dc$  is not zero as we have measured by differential refractometry. We found  $dn/dc = 0.023$  mL/g, while for the previously discussed case of SV-50 in THF we have  $dn/dc = 0.110$  mL/g.

Accordingly, the heterogeneity mode 4 for the toluene solution has a higher relative amplitude than in the case of THF (as has been previously shown<sup>12,48</sup>), and the same holds for modes 1 and 2. The relaxation time of the heterogeneity mode  $\tau_H$  is related to the self-diffusion coefficient  $D_s$  of an A–B diblock copolymer by<sup>46,47</sup>

$$\tau_H^{-1} = q^2 D_s (1 - 2\kappa\chi N c^{1.53}) \quad (12)$$

where  $\chi$  is the interaction parameter between the two polymer blocks A and B and  $\kappa = 2\delta f^2(1-f)^2/(f^2 + (1-f)^2)$ , with  $f$  being the fraction of A blocks and  $\delta = (M_w/M_n) - 1$ . From the data in Figure 4 and eq 12 we obtain a value of the polymer self-diffusion coefficient  $D_s = 6.72 \times 10^{-12}$  m<sup>2</sup>/s where we have used  $M_w/M_n = 1.2$ ,  $f = 0.43$ ,  $\chi = 0.1$ , and  $N = 800$ . PFG NMR measurements on the same solution provide a value for the self-diffusion coefficient of SV-50 in the solution,  $D_{s,NMR} = 6.35 \times 10^{-12}$  m<sup>2</sup>/s, in very good agreement with the value obtained from DLS.

The presence of modes 1 and 2 does not depend on concentration of the polymer, but the relative amplitude of mode 2 increases with increasing polymer concentration. Figure 5 shows that the ratio of amplitudes of mode 2 and 1 (at the same angle), in the absence of any theoretical prediction for mode 2,

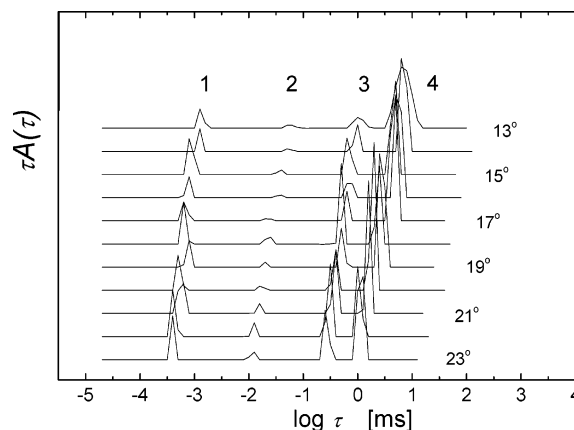


**Figure 4.** Distribution of decay times of the polymer SV-50 in toluene,  $c = 5$  wt %, at the indicated scattering angles.

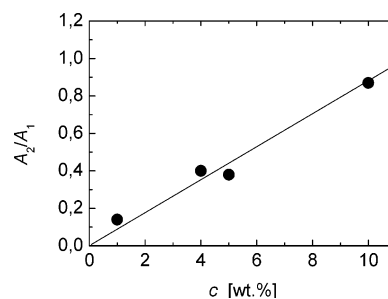


**Figure 5.** Dependence of the ratio of amplitudes  $[A_2/A_1]$  of modes 2 and 1 on the concentration  $c$  (in wt %) of polymer in solution of SV-50 in toluene.

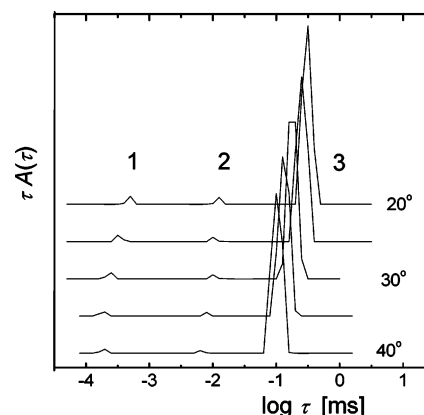


**Figure 6.** Distribution of decay times for a solution of polystyrene PS-97 in toluene,  $c = 5$  wt %.

can be well represented by a linear dependence on concentration. Since in a neat solvent without any polymer mode 1 is also present while mode 2 does not exist (see below), we conclude that the amplitude of mode 2 decreases with decreasing concentration until it vanishes in neat solvent.

**4.2. Homopolymer in a Good Solvent.** Next, we demonstrate that the presence of modes 1 and 2 is not due to the block copolymer character of the polymer. Returning to the simplest possible system of a linear polymer in a good solvent, we show in Figure 6 and Figure 7 the results for a solution of the polystyrene standard PS-97 in toluene at a concentration of 5 and 1 wt % and temperature  $25^\circ\text{C}$ . Modes 1 and 2 are always visible and will be discussed below; mode 3 is the cooperative (translational) diffusion coefficient of the polymer.

In the dilute polystyrene solution (Figure 7) mode 2 is very weak and therefore well observed only at angles below  $20^\circ$  for two reasons: (a) The amplitude of mode 2, according to Figure



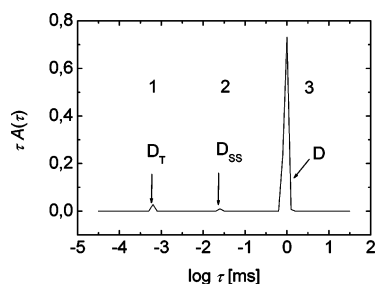


**Figure 7.** Distribution of decay times for a solution of polystyrene PS-97 in toluene,  $c = 1$  wt % at a scattering angle  $17^\circ$ .  $D_T$  is the solvent thermal diffusion coefficient,  $D_{ss}$  is the solvent self-diffusion coefficient, and  $D$  is the polymer translational diffusion coefficient.

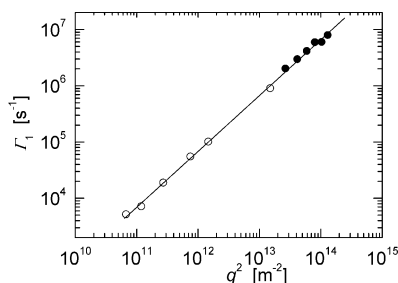


**Figure 8.** Decay rate  $\Gamma_1$  of mode 1 vs  $q^2$  for angles  $1^\circ$ – $15^\circ$  and neat toluene (open circles) and for angles  $20^\circ$ – $45^\circ$  and a PS-97 solution ( $c = 5$  wt %) in toluene (full circles).

5, decreases substantially with decreasing concentration, assuming that the finding in Figure 5 can be applied also for a homopolymer solution. (b) At smaller angles the scattered intensity is higher, and thus the statistics of the correlation function at very small delay times is much better.

## 5. Discussion

The diffusion coefficient corresponding to the decay time of mode 1, for all cases shown in Figures 4, 6, and 7, is  $D = (6\text{--}9) \times 10^{-8}$  m<sup>2</sup>/s, which corresponds very closely to the value of the thermal diffusion coefficient of neat toluene.<sup>49,50</sup> Referring to the experiments performed by Leipertz<sup>23,24</sup> and by Lallemand,<sup>26</sup> who used a heterodyne technique at very small scattering angles, we have investigated the light scattered by neat toluene at very small angles using a homodyne single-mode fiber-optics detection system. Correlation functions obtained at several angles in the range  $1.0^\circ$ – $15^\circ$  show always a single decay. All decay rates obtained on neat toluene together with decay rates of mode 1 in Figure 4 are plotted as a function of  $q^2$  in Figure 8.

A very good linear dependence of the decay rate  $\Gamma_1$  on  $q^2$  is observed in log–log coordinates over 3.5 decades in  $q$  with a slope of 1, confirming the diffusive character of this mode ( $\Gamma_1 = Dq^2$ ). A linear fit to this dependence gives the value of the thermal diffusion coefficient of toluene  $D_T = 8 \times 10^{-8}$  m<sup>2</sup>/s, in good agreement with literature values.<sup>49,50</sup> This demonstrates that the fastest mode 1 observed in Figures 1, 3, 4, 6, and 7 corresponds to the thermal diffusion of the solvent. Since the amplitude of this component does not depend on scattering angle,<sup>11</sup> the contribution of thermal diffusion cannot be neglected in the spectrum of scattered light from polymer solutions when fine details are considered at smaller scattering angles.

The last unidentified dynamic process is mode 2 (defined in Figure 1). It appears in the distributions of decay times in both dilute and semidilute solutions, in block copolymers, and in homopolymers so its origin has to be independent of these characteristics of the polymer/solvent systems. We claim that

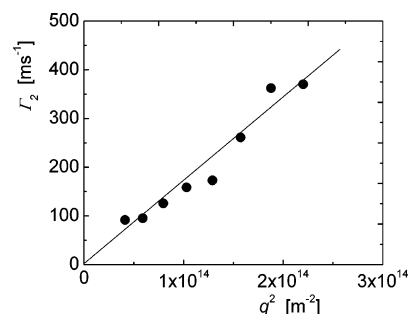


**Figure 9.** Dependence of the decay rate  $\Gamma_2$  of the solvent self-diffusion mode 2 of toluene on  $q^2$ , in a solution of polystyrene PS-97 in toluene at concentration 5 wt %.

**Table 1.** Self-Diffusion Coefficients  $D_{ss}$  (m<sup>2</sup>/s) of Toluene at 25 °C in the Indicated Mixtures

	$D_{ss,NMR}$	$D_{ss}$ from DLS
PS-97/toluene, $c = 5\%$	$1.97 \times 10^{-9}$	$1.93 \times 10^{-9}$
SV-50/toluene, $c = 5\%$	$1.92 \times 10^{-9}$	$2.11 \times 10^{-9}$
toluene- $d_8$ /5% toluene- $h_8$	$2.21 \times 10^{-9}$	$a$
toluene- $d_8$ /20% toluene- $h_8$	$a$	$2.10 \times 10^{-9}$

<sup>a</sup> Not available.

this mode is representative of the self-diffusion of solvent molecules in the polymer solution, and we present several pieces of evidence to support this assertion.

1. The decay rate  $\Gamma_2$  of this mode is proportional to  $q^2$  as is demonstrated in Figure 9; thus, it is a diffusive process.

2. The diffusion coefficient of this process calculated from the decay rate is  $D_{ss} = 1.7 \times 10^{-9}$  m<sup>2</sup>/s, in good agreement with the literature values<sup>51,52</sup> ranging from  $D_{ss} = 1.81 \times 10^{-9}$  to  $2.29 \times 10^{-9}$  m<sup>2</sup>/s obtained by NMR.

3. We have performed PFG NMR measurements on several samples studied also by dynamic light scattering in such a way that the PFG NMR response represents the dynamics of the solvent molecules. Table 1 summarizes the results obtained for solutions of polystyrene PS-97 in toluene, SV-50 in toluene, and neat toluene. Very good agreement between the self-diffusion coefficients of toluene obtained by PFG NMR and DLS is observed both in the solutions and in the neat solvent.

4. A final DLS measurement was performed on a sample of neat toluene. Noticing<sup>53</sup> that toluene has a refractive index of 1.4960 while deuterated toluene- $d_8$  has a refractive index of 1.4930, a mixture of 80 vol % protonated and 20 vol % deuterated toluene was prepared and carefully filtered into a dedusted scattering cell. Although the contrast between protonated and deuterated toluene is extremely small ( $\Delta n = 0.003$ ), it is sufficient to yield a weak but still well-identifiable signal in the correlation function. The latter is shown in Figure 10 together with the corresponding distribution of decay times.

Mode 1 again corresponds to the thermal diffusion of toluene, while the clearly visible mode 2 is the mutual diffusion of deuterated and protonated toluene molecules which is practically equal to the self-diffusion of toluene.<sup>54</sup> The diffusion coefficient corresponding to mode 2 in Figure 10b is  $D_{ss} = 2.1 \times 10^{-9}$  m<sup>2</sup>/s, in very good agreement with the other values of the self-diffusion coefficient of toluene reported above.

Our finding is somewhat unusual in the sense that it is not predicted that solvent self-diffusion should be observed in a dynamic light scattering experiment. We propose the following tentative explanation for our observations. In a neat solvent (toluene) we observed only the thermal diffusion process; we did not observe the self-diffusion process. In order to observe the solvent self-diffusion, contrast has to be created in the system by introducing polymer chains. This is supported by the finding

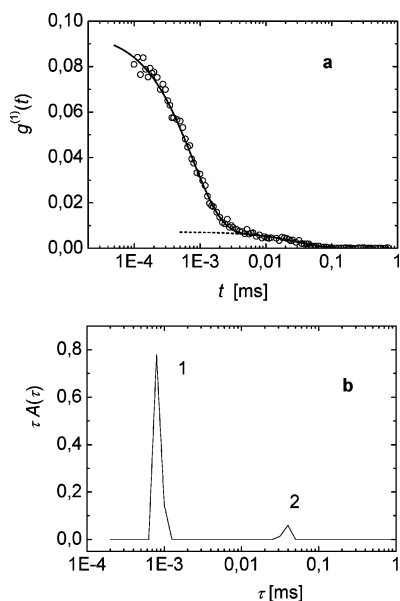


**Figure 10.** Correlation function (a) and distribution of decay times (b) for a mixture of protonated toluene (80 vol %) and deuterated toluene- $d_8$ , at scattering angle  $15^\circ$  and temperature  $25^\circ\text{C}$ . The dashed line in (a) represents the partial correlation function corresponding to mode 2.

that the amplitude of the solvent self-diffusion mode linearly increases with increasing polymer concentration, as shown in Figure 5. When a polymer chain diffuses in the solution, the backflow of solvent molecules compensates for this motion, thereby contributing to fluctuations in dielectric constant. This process appears on a time scale of motion of the solvent molecules.

In the usual treatment of light scattering from macromolecular solutions scattering by solvent molecules is neglected<sup>55,56</sup> because the polarizability of a macromolecule is enormous by comparison to the polarizability of a solvent molecule; this is not compensated by the much larger number of solvent molecules because the solvent structure gives rise to much more destructive interference. It is however noted in ref 55 that macromolecules move much more slowly than the solvent molecules, and therefore their motion should be temporally separable from the solvent motion; this is what we have concluded by analyzing mode 2 in the experiments described above.

## 6. Conclusions

We have shown that a number of different dynamic processes influence the autocorrelation function of light scattered from a polymer solution. The usually described dynamic processes are cooperative or translational diffusion, polymer self-diffusion, and cluster diffusion. Two faster modes have been observed in all cases of dilute and semidilute solutions of a homopolymer and a diblock copolymer. The fastest mode has a diffusion coefficient of the order of  $10^{-8}\text{ m}^2/\text{s}$  and corresponds to the thermal diffusion of the solvent. This mode has been observed also in neat solvent. The slower of these fast modes is also diffusive with a diffusion coefficient (order of  $10^{-9}\text{ m}^2/\text{s}$ ) equal to that obtained by PFG NMR and corresponds to the self-diffusion of the solvent. Although this mode is not predicted by the theory of light scattering from polymer solutions, we have presented four experiments that support our findings. While we do not attempt to derive a more detailed theory of light scattering from polymer solutions, we point to approximations made in the usual description of scattered light that may be at

the origin of the lack of theoretical description of this process. We hope that further theoretical developments could clarify this issue in a similar way as when the theoretically unpredicted but experimentally observed self-diffusion of diblock copolymer molecules in solution was explained by inclusion of polymer chain composition heterogeneity.<sup>47</sup>

**Acknowledgment.** This work was supported by the Grant agency of the Academy of sciences of the Czech Republic (Grant A4050403).

## References and Notes

- (1) Cummins, H. Z. In *Photon Correlation and Light Spectroscopy*; Cummins, H. Z., Pike, E. R., Eds.; Proc. NATO Advanced Study Institute, Capri, Italy, 1973.
- (2) Patterson, G. D.; Munoz-Rojas, A. *Annu. Rev. Phys. Chem.* **1987**, *38*, 191.
- (3) Štěpánek, P.; Koňák, Č.; Jakeš, J. *Polym. Bull. (Berlin)* **1986**, *16*, 67.
- (4) Schätzel, K. In *Dynamic Light Scattering: The Method and Some Applications*; Brown, W., Ed.; Oxford Science Publications: Oxford, 1993.
- (5) Ostrowski, N.; Sornette, D.; Parker, P.; Pike, E. R. *Opt. Acta* **1981**, *28*, 1059–1070.
- (6) McWhirter, J. G. *Opt. Acta* **1980**, *27*, 83.
- (7) Bertero, M.; Brianzi, P.; Pike, E. R.; de Villiers, G.; Lan, K. H.; Ostrowski, N. *J. Chem. Phys.* **1985**, *82*, 1551.
- (8) *Dynamic Light Scattering: The Method and Some Applications*; Brown, W., Ed.; Oxford Science Publications: Oxford, 1993.
- (9) *Light Scattering: Principles and Development*; Brown, W., Ed.; Oxford Science Publications: Oxford, 1996.
- (10) *Scattering in Polymeric and Colloidal Systems*; Brown, W., Mortensen, K., Eds.; Gordon and Breach Science Publishers: Langhorne, PA, 2000.
- (11) Berne, B. J.; Pecora, R. *Dynamic Light Scattering*; Dover Publications: New York, 2000.
- (12) Pan, C.; Maurer, W.; Lu, Z.; Lodge, T. P.; Štěpánek, P.; von Meerwal, E. D.; Watanabe, H. *Macromolecules* **1995**, *28*, 1889.
- (13) Štěpánek, P.; Lodge, T. In *Light Scattering: Principles and Development*; Brown, W., Ed.; Oxford Science Publications: Oxford, 1996.
- (14) Štěpánek, P.; Brown, W. *Macromolecules* **1998**, *31*, 1889.
- (15) Adam, M.; Delsanti, M. *Macromolecules* **1985**, *18*, 1760.
- (16) Nicolai, T.; Brown, W. In *Light Scattering: Principles and Development*; Brown, W., Ed.; Oxford Science Publications: Oxford, 1996.
- (17) Borsali, R.; Giebel, L.; Fischer, E. W.; Meier, G. *J. Non-Cryst. Solids* **1991**, *131*, 816.
- (18) Kanaya, T.; Patkowski, A.; Fischer, E. W.; Seils, J.; Glaser, H.; Kaji, K. *Macromolecules* **1995**, *28*, 7831.
- (19) Semenov, A. N. *Physica A* **1990**, *166*, 263.
- (20) Boudenne, N.; Anastasiadis, S. H.; Fytas, G.; Xenidou, M.; Hadjichristidis, N.; Semenov, A. N.; Fleischer, G. *Phys. Rev. Lett.* **1996**, *77*, 506.
- (21) Floudas, G.; Štěpánek, P. *Macromolecules* **1998**, *31*, 6951.
- (22) Floudas, G.; Placke, P.; Štěpánek, P.; Brown, W.; Fytas, G.; Ngai, K. *Macromolecules* **1995**, *28*, 6799.
- (23) Fröba, A. P.; Will, S.; Leipertz, A. *Int. J. Thermophys.* **2000**, *21*, 603.
- (24) Will, S.; Leipertz, A. *Int. J. Thermophys.* **2001**, *22*, 317.
- (25) Sidebottom, D. L.; Sorensen, C. M. *Phys. Rev. B* **1989**, *40*, 461.
- (26) Allain, C.; Lallemand, P. *J. Phys. (Paris)* **1979**, *40*, 693.
- (27) Köhler, W.; Fytas, G.; Steffen, W.; Reinhardt, L. *J. Chem. Phys.* **1996**, *104*, 248.
- (28) Gulari, E.; Brown, R. J.; Pings, C. J. *AIChE J.* **1973**, *19*, 1196.
- (29) Gulari, E.; McKeigue, K. *J. Phys. Chem.* **1984**, *88*, 3472.
- (30) Czworniak, K. J.; Andersen, H. C.; Pecora, R. *Chem. Phys.* **1975**, *11*, 451.
- (31) Štěpánek, P.; Tuzar, Z.; Nallet, F.; Noirez, L. *Macromolecules* **2005**, *38*, 3426.
- (32) Tanford, C. *Physical Chemistry of Macromolecules*; J. Wiley & Sons: New York, 1961.
- (33) Jakeš, J. *Collect. Czech. Chem. Commun.* **1995**, *60*, 1781.
- (34) Štěpánek, P. In *Dynamic Light Scattering: The Method and Some Applications*; Brown, W., Ed.; Oxford Science Publications: Oxford, 1993.
- (35) Štěpánek, P.; Johnsen, R. M. *Collect. Czech. Chem. Commun.* **1995**, *60*, 1941.
- (36) Štěpánek, P.; Lodge, T. P. *Macromolecules* **1996**, *29*, 1244.
- (37) Jakeš, J. *Czech. J. Phys.* **1988**, *B38*, 1305.
- (38) Provencher, S. W. In *Laser Light Scattering in Biochemistry*; Harding, S. E., Sattelle, D. B., Bloomfield, V. A., Eds.; Royal Society of Chemistry: London, 1992.

- (39) de Gennes, P. G. *Scaling Concepts in Polymer Physics*; Cornell University Press: Ithaca, NY, 1979.
- (40) Adam, M.; Delsanti, M. *J. Phys., Lett.* **1984**, *45*, L279.
- (41) Adam, M.; Delsanti, M. *Macromolecules* **1977**, *10*, 1229.
- (42) Balsara, N. P.; Štěpánek, P.; Lodge, T. P.; Tirrell, M. *Macromolecules* **1991**, *24*, 6227.
- (43) Anastasiadis, S. H.; Fytas, G.; Vogt, S.; Gerharz, B.; Fischer, E. W. *Europhys. Lett.* **1993**, *22*, 619.
- (44) Liu, Z.; Kobayashi, K.; Lodge, T. P. *J. Polym. Sci., Part B: Polym. Phys.* **1998**, *36*, 1831.
- (45) Pham, K. N.; Egelhaaf, S. U.; Pusey, P. N.; Poon, W. C. K. *Phys. Rev. E* **2004**, *69*, 11503.
- (46) Semenov, A. N.; Fytas, G.; Anastasiadis, S. H. *Polym. Prepr. (Am. Chem. Soc., Div. Polym. Chem.)* **1994**, *35* (1), 618.
- (47) Jian, T.; Anastasiadis, S. H.; Semenov, A. N.; Fytas, G.; Adachi, K.; Kotaka, T. *Macromolecules* **1994**, *27*, 4762.
- (48) Liu, Z.; Pan, C.; Štěpánek, P.; Lodge, T. P. *Macromolecules* **1995**, *28*, 3221.
- (49) Will, S.; Leipertz, A. *Int. J. Thermophys.* **2001**, *22*, 317.
- (50) Kraft, K.; Matos, Lopes, M.; Leipertz, A. *Int. J. Thermophys.* **1995**, *16*, 423.
- (51) O'Reilly, D. E.; Peterson, E. M. *J. Chem. Phys.* **1972**, *56*, 2262.
- (52) Kim, J. H.; Lee, S. H. *Bull. Korean Chem. Soc.* **2002**, *23*, 441.
- (53) *Handbook of Fine Chemicals*; Aldrich: Milwaukee, WI, 2005.
- (54) Felderhof, B. U. *J. Chem. Phys.* **2003**, *118*, 11326.
- (55) Chapter 5.3 in ref 11.
- (56) Jones, R. B.; Pusey, P. N. *Annu. Rev. Phys. Chem.* **1991**, *42*, 137, section 3.

MA0620518